

# Controlling Conformations of Diketopyrrolopyrrole-Based Conjugated Polymers: Role of Torsional Angle

Catherine Kanimozhi,<sup>†</sup> Mallari Naik,<sup>†</sup> Nir Yaacobi-Gross,<sup>‡</sup> Edmund K. Burnett,<sup>§</sup> Alejandro L. Briseno,<sup>§</sup> Thomas D. Anthopoulos,<sup>‡</sup> and Satish Patil\*,<sup>†</sup>

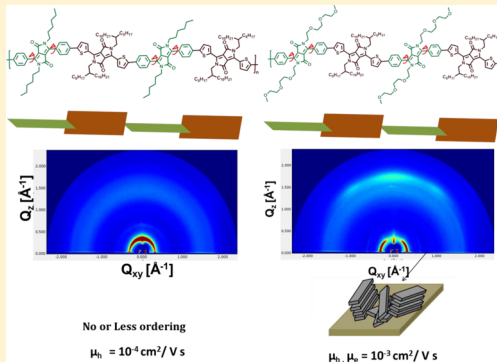
<sup>†</sup>Solid State and Structural Chemistry Unit, Indian Institute of Science, Bangalore 560012, India

<sup>‡</sup>Department of Physics and Centre for Plastic Electronics, Blackett Laboratory, Imperial College London, London SW7 2BW, United Kingdom

<sup>§</sup>Department of Polymer Science and Engineering, University of Massachusetts, Amherst, Massachusetts 01003, United States

## Supporting Information

**ABSTRACT:** Transport of charge carriers through conjugated polymers is strongly influenced by the presence and distribution of structural disorders. In the present work, structural defects caused by the presence of torsional angle were investigated in a diketopyrrolopyrrole (DPP)-based conjugated polymer. Two new copolymers of DPP were synthesized with varying torsional angles to trace the role of structural disorder. The optical properties of these copolymers in solution and thin film reveal the strong influence of torsional angle on their photophysical properties. A strong influence was observed on carrier transport properties of polymers in organic field-effect transistors (OFET) device geometry. The polymers based on phenyl DPP with higher torsional angle (PPTDPP-OD-TEG) resulted in high threshold voltage with less charge carrier mobility as compared to the polymer based on thiophene DPP (2DPP-OD-TEG) bearing a lower torsional angle. Carrier mobility and the molecular orientation of the conjugated polymers were correlated on the basis of grazing incidence X-ray scattering measurements showing the strong role of torsional angle introduced in the form of structural disorder. The results presented in this Article provide a deep insight into the sensitivity of structural disorder and its impact on the device performance of DPP-based conjugated polymers.



## INTRODUCTION

The electronic properties of  $\pi$ -conjugated polymers are distinctly different from those of conventional inorganic semiconductors. The unique properties of conjugated polymers, solution processability, low cost, flexibility, and tunable band gap, fascinated the world of organic semiconductors.<sup>1</sup> However, the performance of these materials in optoelectronic devices severely suffers due to the low mobility of charge carriers. The charge carrier transport in conjugated polymers is strongly influenced by many factors such as  $\pi$ -conjugation length, intermolecular interactions, and  $\pi-\pi$  stacking, which depend on the planarity of the polymer chain.<sup>2–4</sup> The anisotropy in charge carrier transport points out that any defects in the form of bends or twists in the polymer chain affect the coplanarity of the polymer backbone and can be detrimental for the device performance.<sup>5–7</sup> Defects mainly arise due to the presence of tetrahedral carbon within the polymer chain, or the torsional angle may cause defects in the form of ring-rotational order.<sup>8</sup> In the recent past, there is an immense improvement in the device performance especially in organic solar cells and field-effect transistors, but there is a lack of information to understand the fundamental properties that strongly influence the performance of optoelectronic devices.

One such effect is the heterogeneity of chain conformation of polymers in thin film.<sup>9–12</sup> The physical and electronic properties of conjugated polymers are very sensitive toward the conformation adopted by the polymer chain in a given solvent.<sup>13–15</sup> Despite this complex heterogeneity of polymer chain conformations, the performance of conjugated polymers in optoelectronic devices has improved rapidly; especially the power conversion efficiency of organic solar cells dramatically improved from 1% to 9%.<sup>16,17</sup> These advances in the area of flexible electronics are accomplished by excellent molecular engineering and by the development of a new class of low band gap conjugated polymers.<sup>18</sup>

In this regard, conjugated polymers based on a diketopyrrolopyrrole (DPP) core have received enormous attention due to their versatile photophysical and electronic properties obtained by coupling various aromatic and heteroaromatic moieties.<sup>19</sup> Phenyl, thiophene, furan, and thieno-thiophene-based DPP materials have been exploited innumerable, and a library of polymers showing desired properties and devices with

Received: February 12, 2014

Revised: April 28, 2014

Published: May 21, 2014



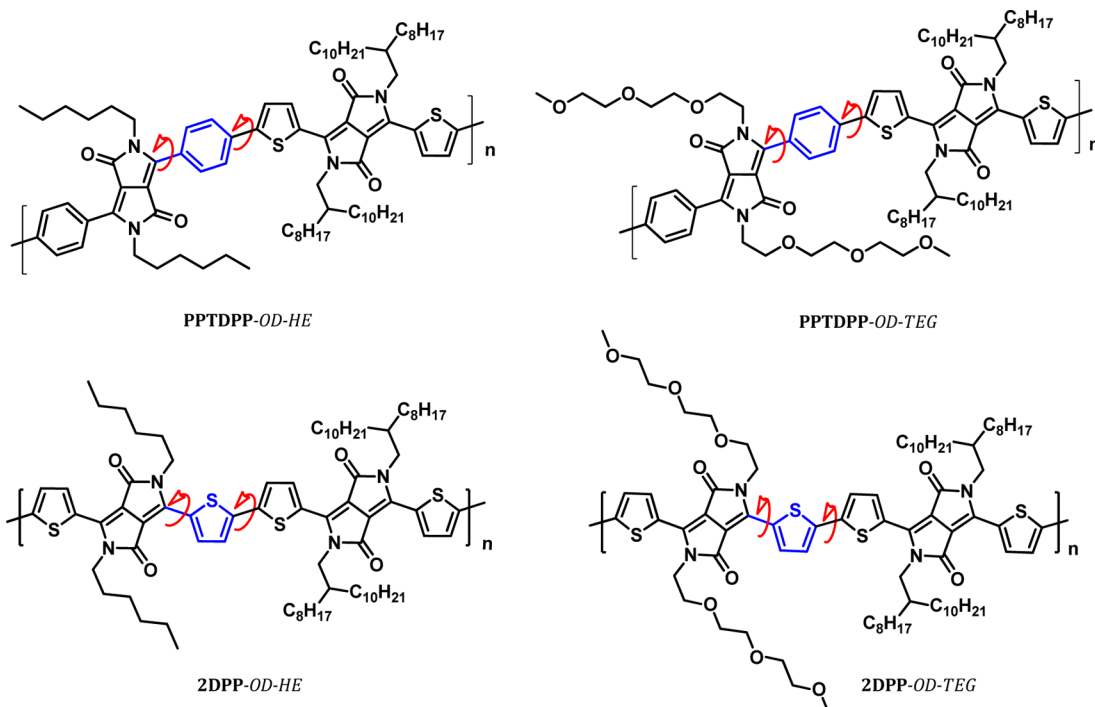
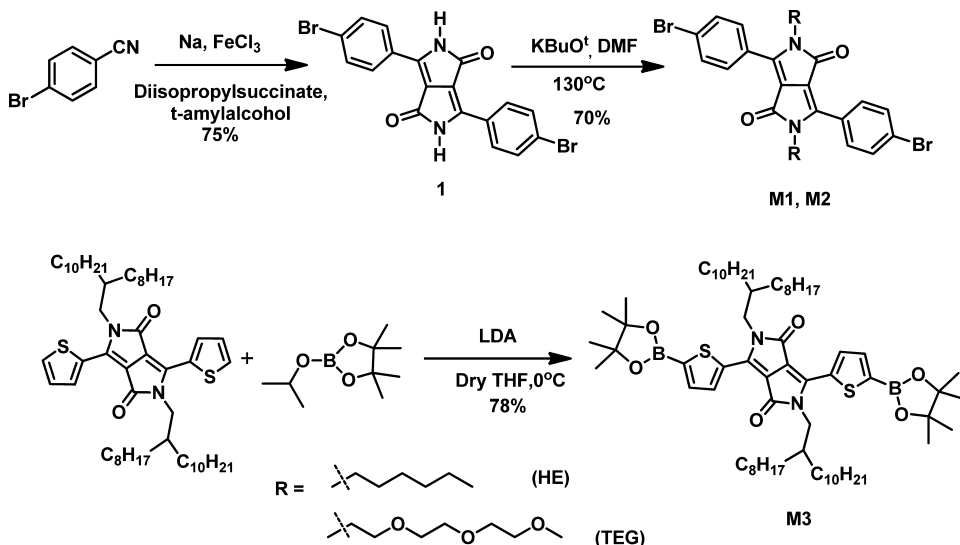


Figure 1. Chemical structure of DPP–DPP copolymers.

**Scheme 1. Synthesis of Monomers M1, M2, and M3**

efficiencies up to 8–9% has been reported.<sup>20–24</sup> Charge carrier mobility of  $\sim 10 \text{ cm}^2 \text{ V}^{-1} \text{ s}^{-1}$  have also been achieved using DPP-based solution processable polymer in OTFTs.<sup>25,26</sup> However, there is a gap in understanding the high performance of these materials with respect to their structural properties. The influence of structural disorders on ring torsion has been seldom investigated. A structural disorder plays a critical role in controlling the charge-carrier mobility, as ring rotations could force a deviation from planarity of the polymer chain.

Motivated by these questions, we focused on investigating the role of torsional angle in DPP-based copolymers with respect to their electronic and structural properties. We rationally synthesized two new DPP–DPP-based conjugated copolymers to study the influence of torsional angle on device performance and optical properties. Chemical structures of the

synthesized DPP–DPP polymers, PTPDPP-OD-HE and PPTDPP-OD-TEG, based on phenyl DPP are shown in Figure 1. To emphasize the importance of the torsional angle on the rotational degree of freedom of the polymer chain, chemical structures of TDPP–TDPP copolymers (2DPP-OD-HE, 2DPP-OD-TEG)<sup>27</sup> based on thiophene DPP are also shown in Figure 1.

The OFET characteristics of the DPP copolymers (PPTDPP-OD-HE and PPTDPP-OD-TEG) were correlated with the morphology and crystallinity of the films. Copolymers exhibit ambipolar FET characteristics with mobilities in the order of  $10^{-3}$ – $10^{-4} \text{ cm}^2 \text{ V}^{-1} \text{ s}^{-1}$ . Single crystals of the monomers were grown to manifest the intermolecular interactions and coplanarity of the conjugated plane in monomers. Grazing incidence X-ray diffraction (GIXD)

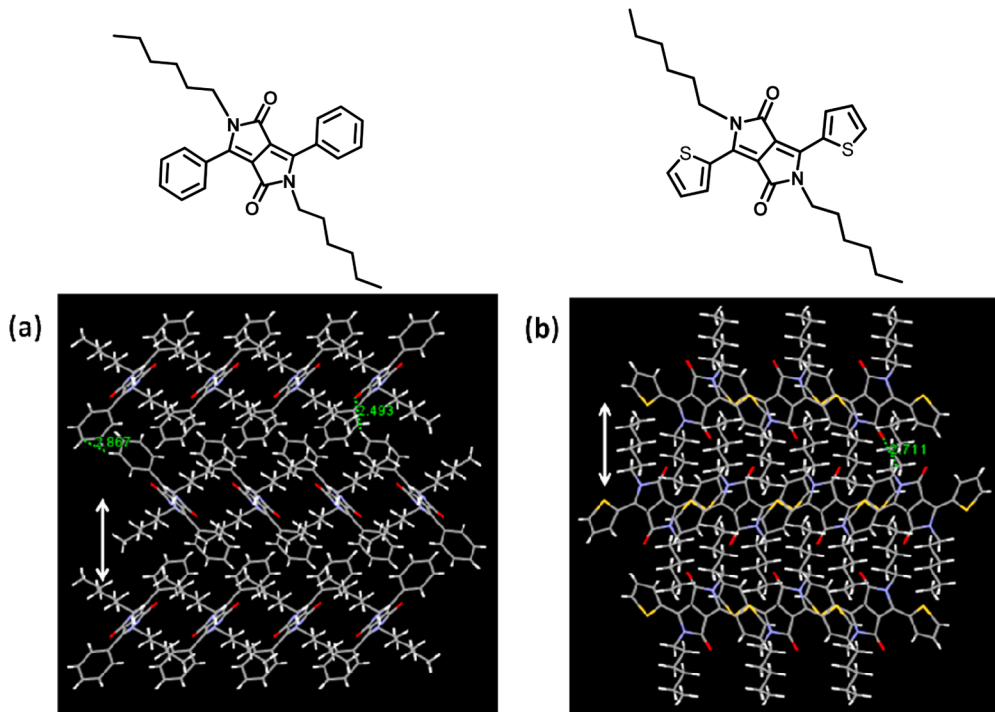


**Figure 2.** Crystal structures of (a) PDPP-Hex and (b) TDPP-Hex.

provided the insight into understanding the degree of packing, long-range ordering, and orientation of the polymer crystallites on the substrate surface. As a result of smaller torsional angle and the preferential orientation of the polymer crystallites, TDPP-based polymers **2DPP-OD-HE** and **2DPP-OD-TEG**<sup>27</sup> exhibited improved charge carrier mobilities with lower threshold voltages as compared to phenyl DPP-based polymers **PPTDPP-OD-HE** and **PPTDPP-OD-TEG**. This work highlights the importance of chain conformations of conjugated polymers that result from torsional defects. In addition, our results show that the transport of carriers in semiconducting polymers is extremely sensitive to a diverse range of disorders including torsional angle between structural subunits of the donor–acceptor bridge.

## RESULTS AND DISCUSSION

### Synthesis of Monomers and Single Crystal Studies.

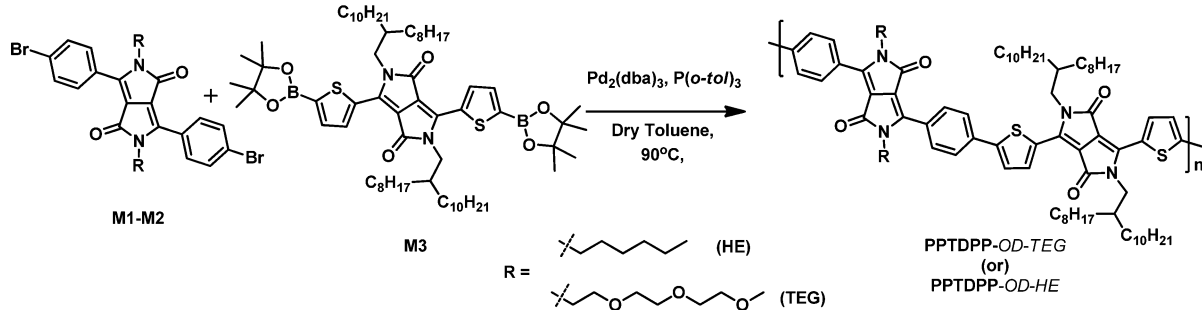
The synthetic pathway for the monomers **M1–M3** is outlined in Scheme 1. All monomers were synthesized according to previously reported procedures.<sup>28</sup> The diketopyrrolopyrrole core was synthesized by a pseudo Stobbe condensation using diisopropyl succinic ester and *p*-bromo benzonitrile (PDPP) (or) 2-thiophene carbonitrile (TDPP) in the presence of a strong base sodium *tert*-amyl alkoxide.<sup>29</sup>

The role of ring torsions in monomers is investigated by growing single crystals of model compounds **PDPP-Hex** and **TDPP-Hex**. The single crystals of monomers (**PDPP-Hex** and **TDPP-Hex**) were grown from a dichloromethane:methanol (8:2 v/v) solution. Chemical structures and the corresponding crystal structures of *n*-hexyl side chain substituted **PDPP-Hex** and **TDPP-Hex** are shown in Figure 2. Single crystal analysis of **PDPP-Hex** and **TDPP-Hex** affords a systematic insight into the torsion induced by phenyl and thiophene ring in the donor–acceptor bridge of DPP. The crystallographic data, solid-state packing, and refinement are given somewhere else.<sup>30</sup> Both **PDPP-Hex** and **TDPP-Hex** crystallized in a monoclinic

crystal system with a space group of  $P2_1/c$ . A distinct difference in backbone planarity between **PDPP-Hex** and **TDPP-Hex** was observed. In **PDPP-Hex**, the phenyl rings are twisted and found to be out of plane with the lactam unit. The repulsive interaction between the *ortho*-hydrogens of phenyl ring and the alkyl chain of lactam unit results in a torsional angle of  $35^\circ$  (Figure 2). In contrast, **TDPP-Hex** displays a torsional angle close to  $10^\circ$ , due to the absence of the repulsive interaction between thiophene and the lactam unit. This deviation from planarity in **PDPP-Hex** strongly influences crystal packing, intermolecular  $\pi$ – $\pi$  interactions, and electronic coupling between the donor and acceptor unit as shown in Figure 2.

Distinct molecular ordering is observed in the packing diagram for phenyl and thiophene substituted DPP molecules due to the torsional angle difference. The molecular packing in **PDPP-Hex** is driven by the intermolecular hydrogen (C–H…O) bonding between the C=O of the lactam ring and the phenyl ring (C–H) from the neighboring molecule with a distance of 2.5 Å. Similar C–H…O intermolecular hydrogen bonding was observed in **TDPP-Hex** molecular packing between C=O of the lactam ring and the thiophene ring from the neighboring molecule with a distance of 2.7 Å. **PDPP-Hex** exhibited a herringbone molecular packing (along the *a* axis) with a slipped  $\pi$ -stacking arrangement where the torsion between the phenyl rings pushes the molecules apart, preventing closer packing. The packing diagram of **TDPP-Hex** shows an improved  $\pi$ -stacking interaction with a similar herringbone-like packing. Favorable interdigititation of substituted *n*-hexyl chains in **TDPP-Hex** allows strong  $\pi$ -interaction between the thiophene rings (Figure 2), indicating the small torsional angle allows for close packing of the neighboring molecules. The twist or the torsional angle introduced in each repeating unit will have major implications in electronic and structural properties of the resulting polymer. With this objective, we carried out polymerization by coupling **PDPP-TDPP**, and the results are discussed below.

Scheme 2. Synthesis of Copolymers PPTDPP-OD-HE and PPTDPP-OD-TEG



**Synthesis of Polymers and Photophysical Properties.** The synthesis of the copolymers PPTDPP-OD-HE and PPTDPP-OD-TEG is shown in Scheme 2. These polymers were synthesized by a Suzuki-cross-coupling reaction between monomer M1 or M2 and M3 in the presence of a palladium catalyst  $\text{Pd}_2(\text{dba})_3$  with an active ligand  $\text{P}(o\text{-tol})_3$ . The crude polymer was then precipitated in methanol and further purified through Soxhlet extraction. The average molecular weights and polydispersity index were measured from gel permeation chromatography (GPC) using a polystyrene standard. Both polymers exhibit number-average molecular weights ( $M_n$ ) greater than  $35 \text{ kg mol}^{-1}$  with a polydispersity index (PDI) in the order of 3.0 as given in Table 1. The polymers are highly

Table 1. Molecular Weight of the Copolymers

polymer	$M_n$ (kg/mol)	$M_w$ (kg/mol)	PDI ( $M_w/M_n$ )	$T_d$ (°C)
PPTDPP-OD-HE	37.3	78.1	2.21	370
PPTDPP-OD-TEG	35.1	131	3.72	355

soluble (>20 mg/mL) in common organic solvents such as chloroform, dichloromethane, and tetrahydrofuran at room temperature. Structural characterization of the monomers and polymers was carried out using  $^1\text{H}$  NMR,  $^{13}\text{C}$  NMR, IR, and mass spectrometry.

The sensitivity to structural disorder is also manifest in the optical properties of the DPP-based copolymers. The UV-visible absorption spectra of the copolymers PPTDPP-OD-HE

and PPTDPP-OD-TEG in chloroform and a thin film are shown in Figure 3a. The detailed optical data of the polymers are summarized in Table 2. Both polymers exhibit a low energy band and a high energy band with well-defined vibronic features. The high energy peak between 280 and 420 nm corresponds to  $\pi-\pi^*$  transition, and the low energy peak between 480 and 700 nm corresponds to the strong intermolecular interaction from the donor to the central acceptor (DPP) unit. As compared to the solution state absorption spectra, the thin film absorption spectra showed a red shift and spectral broadening, which can be attributed to the strong electronic coupling and enhanced  $\pi-\pi$  interactions in the solid state.

This role of torsion angle has been exemplified by comparing the UV-visible spectra for the polymers based on thiophene DPP (2DPP-OD-HE and 2DPP-OD-TEG). The UV-visible absorption spectra of the copolymers 2DPP-OD-HE and 2DPP-OD-TEG thin films are shown in Figure 3b. A prominent red-shift of  $\geq 250$  nm in TDPP-based polymers reveals the strong electronic coupling of the donor and acceptor. The spectral broadening in 2DPP-OD-HE and 2DPP-OD-TEG also suggests the association of strong intermolecular solid state interactions as compared to PPTDPP-OD-HE and PPTDPP-OD-TEG. The enhanced repulsion between neighboring rings of the donor–acceptor in PDPP observed from the single crystal study increases the average ring-torsional angle, and decreases the electronic coupling, thus influencing the optical band gap of the polymers. The optical band gap of these polymers was obtained from the

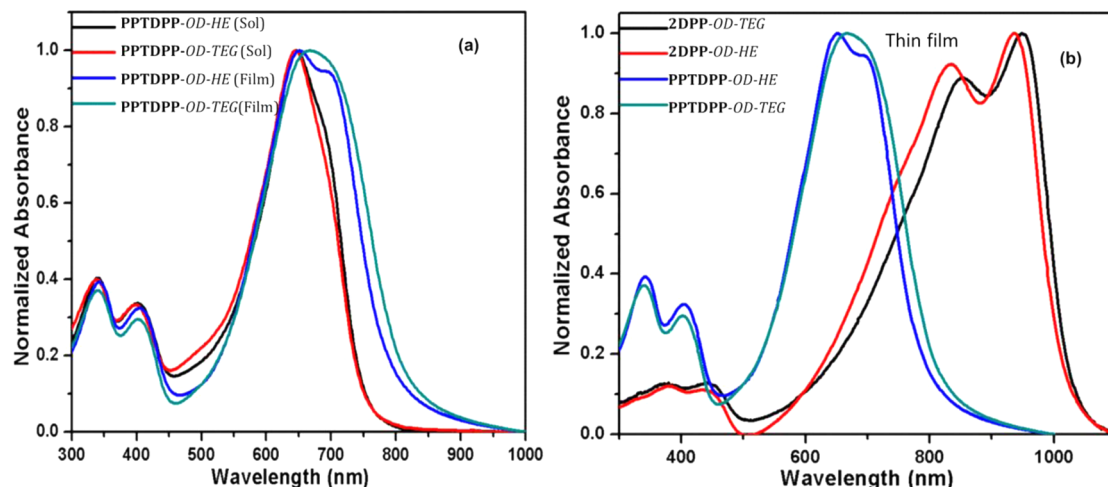


**Figure 3.** (a) UV-visible absorption spectra of copolymers PPTDPP-OD-HE and PPTDPP-OD-TEG in chloroform and thin film. (b) Comparison of UV-visible absorption spectra of the copolymers 2DPP-OD-HE, 2DPP-OD-TEG, PPTDPP-OD-HE, and PPTDPP-OD-TEG in thin films.<sup>21</sup>

Table 2. Photophysical and Electrochemical Properties of the Copolymers

polymer	UV-vis absorption spectra			electrochemical properties			
	solution	thin film		$E_g^{\text{opt}}$ (eV)	$E_{\text{ox}}^{\text{onset}}$ (v)	HOMO (eV)	LUMO <sup>a</sup> (eV)
PPTDPP-OD-HE	650	660	800	1.55	0.91	-5.33	-3.78
PPTDPP-OD-TEG	658	670	832	1.49	0.77	-5.26	-3.71

<sup>a</sup>Calculated by subtracting optical band gap from HOMO.

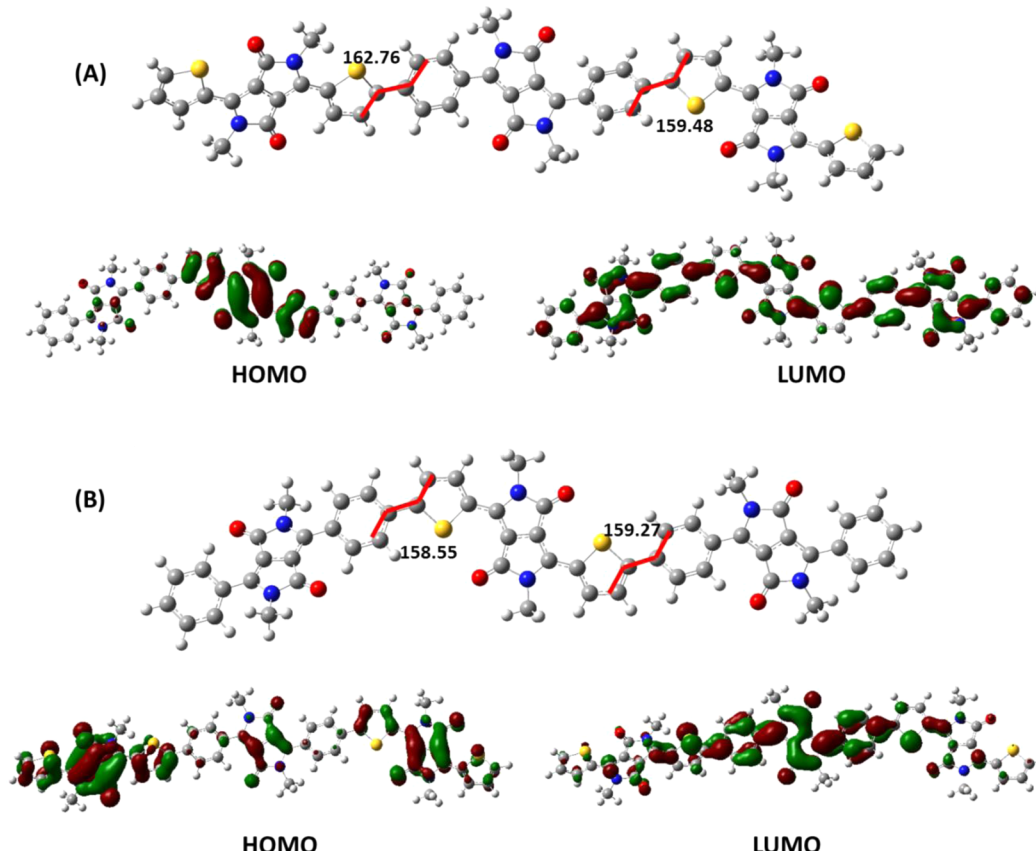


Figure 4. Optimized geometry for the model trimers (A) TPT and (B) PTP of the polymer PPTDPP-OD-ME.

absorption edge of the film of each polymer. 2DPP-OD-HE and 2DPP-OD-TEG exhibit a low band gap of  $\sim 1.2$  eV as compared to PPTDPP-OD-HE and PPTDPP-OD-TEG, which show a higher band gap of  $\sim 1.6$  eV.

The electronic structure and molecular geometry were investigated by using density functional theory (DFT) calculations. Methyl group substituted DPP trimers were considered to minimize the computational efforts. The growing polymer chain constitutes two types of alternate units of PDPP and TDPP. Assuming these possible structures, two types of trimers chemical structures (TPT and PTP) were considered as model compounds to optimize the ground-state geometry. TPT contains a central core as PDPP coupled with TDPP, whereas PTP is coupled with PDPP. All of the quantum-chemical calculations were carried out using DFT with the B3LYP hybrid function and 6-31G (d+)\* basis set as implemented in Gaussian 03. The energy minimized geometry of the model trimer and torsional angles are shown in Figure 4.

It can be seen from the side view that the trimer backbone is tilted from coplanarity with torsional angles of  $20^\circ$  as compared to the polymers based on thiophene DPP where a small torsional angle of  $2^\circ$  was observed between neighboring DPP

units.<sup>27</sup> Unlike the thiophene DPP-based polymers, the HOMO and LUMO orbitals are localized on either of the DPP units showing the weak orbital overlapping. This could be due to an increase in the torsional angle, which deviates the conjugated aromatic backbone from coplanarity. The simulated optical absorption spectrum for the trimer unit of the polymers (not shown here) PPTDPP-OD-HE and PPTDPP-OD-TEG well correlates with the experimental observation that the absorption maximum lies in the high energy regime as compared to the polymers based on thiophene DPP (Figure 3b).

**Electrochemical Properties.** Cyclic voltammetry was employed to estimate the oxidation, reduction potentials, and HOMO–LUMO energy levels of each polymer. Cyclic voltammograms of PPTDPP-OD-HE and PPTDPP-OD-TEG are shown in Figure 5, and the data are tabulated in Table 2. Both polymers exhibit reversible oxidation cycles. Platinum electrodes were used as working and counter electrode, where  $\text{Ag}/\text{Ag}^+$  was employed as a reference electrode. The energy levels calibrated with an internal standard ferrocene/ferrocenium redox couple ( $\text{Fc}/\text{Fc}^+$ ), and HOMO levels were deduced from eq 1.

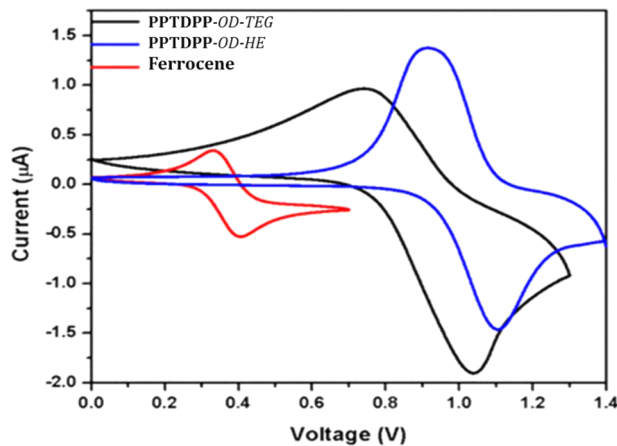


**Figure 5.** Cyclic voltammograms of the polymers PPTDPP-OD-HE and PPTDPP-OD-TEG with a scan rate of  $20 \text{ mV s}^{-1}$ .

$$E_{\text{HOMO}} = -(E_{\text{onset}}^{\text{ox}} + 4.8 - E_{\text{Fc/Fc+}}^{\text{ox}}) \text{ eV} \quad (1)$$

where  $E_{\text{onset}}^{\text{ox}}$  is the oxidation onset.

The oxidation onsets were 0.91 and 0.77 V, giving HOMO energies of 5.33 and 5.26 eV for PPTDPP-OD-HE and PPTDPP-OD-TEG, respectively. DPP containing polymers with effective overlap between donor and acceptors are known to have high lying HOMOs;<sup>13,31</sup> however, a low lying HOMO was observed, suggesting poor electronic overlap of the donor and acceptor. LUMO levels of the polymers were calculated using the difference between the optical band gap ( $E_{\text{opt}}$ ) and HOMO level obtained from electrochemical measurements and were found to be 3.78 and 3.71 eV for PPTDPP-OD-HE and PPTDPP-OD-TEG, respectively.

**Organic Field-Effect Transistor Measurements.** To investigate the charge transport properties of these polymers, OFET devices were fabricated using a bottom-gate, bottom-contact (BG-BC) device configuration. BG-BC devices were fabricated using Si/SiO<sub>2</sub> as the gate electrode/dielectric layers, with photolithographically prepatterned Au source/drain electrodes. The organic semiconductor layer was then spun cast on the substrates to complete the transistor fabrication. The devices were then thermally annealed at different temperatures (80, 140, and 160 °C) under nitrogen atmosphere. Output and transfer characteristics for BG-BC transistors based on PPTDPP-OD-TEG and PPTDPP-OD-HE polymers are shown in Figures 6 and 7, respectively. PPTDPP-OD-TEG devices exhibit clear ambipolar characteristics (Figure 6) with electron and hole mobilities in the order of  $10^{-3} \text{ cm}^2 \text{ V}^{-1} \text{ s}^{-1}$ . Mobility in the saturated regime was extracted using eq 2:

$$I_{\text{DS}} = \frac{W \mu_{\text{FE}} C_{\text{ox}}}{L} (V_G - V_t)^2 \quad (2)$$

where  $I_{\text{DS}}$  is the source-drain current,  $V_G$  is the applied gate voltage,  $V_t$  is the threshold voltage of the device,  $W$  is the channel width,  $L$  is the channel length,  $C_{\text{ox}}$  is the geometrical capacitance of the oxide gate dielectric used, and  $\mu_{\text{FE}}$  is the field-effect charge carrier mobility. The threshold voltage ( $V_t$ ) was extracted from the saturation regime using the intercept of the extrapolated linear part of the  $I_{\text{DS}}^{1/2}$  with the  $V_G$  axis at  $I_{\text{DS}} = 0$ . The on/off ratio of the channel current was calculated as the ratio of the current measured at  $V_{\text{DS}} \geq 30 \text{ V}$  and  $V_G = 0 \text{ V}$  yielding values on the order of  $10^3$ .

Transistors based on PPTDPP-OD-HE exhibited hole mobility in the order of  $10^{-4} \text{ cm}^2 \text{ V}^{-1} \text{ s}^{-1}$ . Comparable charge

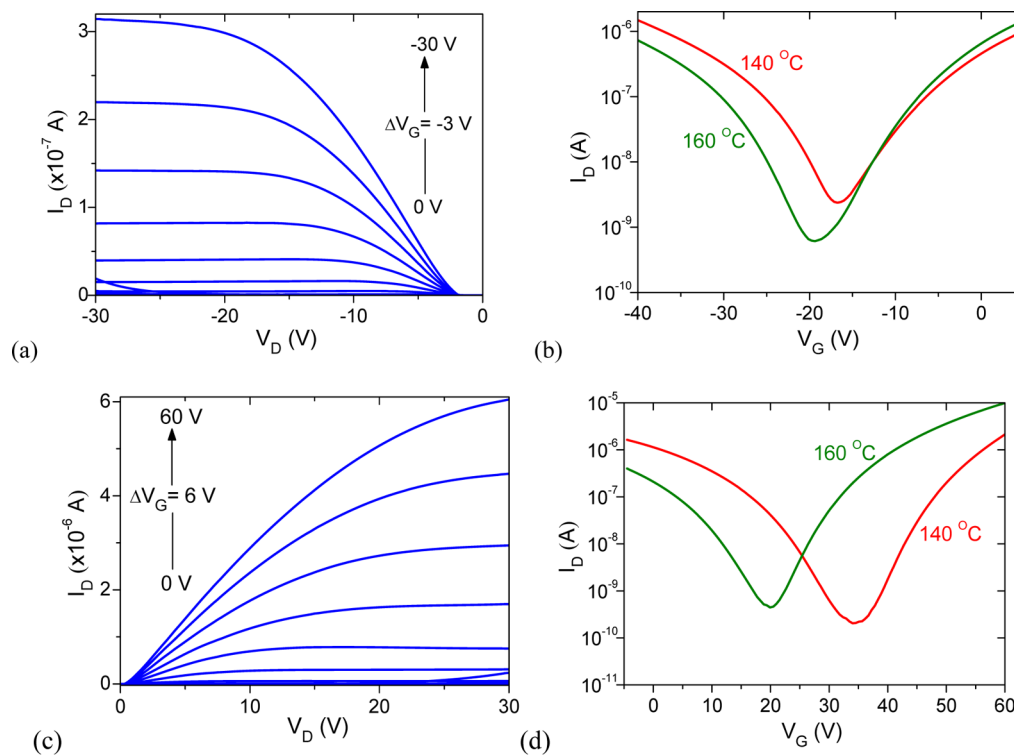


**Figure 6.** Output and transfer characteristics of PPTDPP-OD-TEG-based BG-BC transistors. (a,b) Output and transfer curves, respectively, measured in p-channel operation. (c,d) Output and transfer curves, respectively, measured in n-channel operation. Transfer curves were measured at  $V_D = \pm 30 \text{ V}$ . (d) All measurements reveal clear ambipolar transistor operation with comparable hole and electron currents.

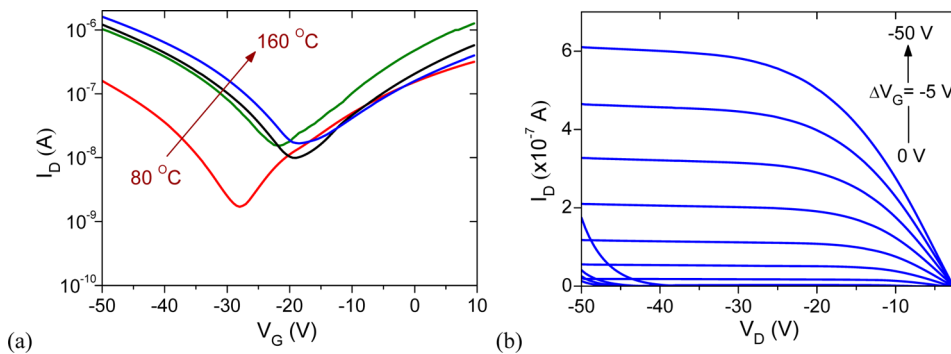


**Figure 7.** Transfer (a) and output (b) characteristics measured for BG-BC transistors based on the copolymer PPTDPP-OD-HE. Transfer curves were measured at  $V_D = 50$  V.

**Table 3. Summary of the Polymer-Based Transistor Parameters**

polymer	device config	D/S	gate dielectric	$\mu_e$ ( $\text{cm}^2 \text{V}^{-1} \text{s}^{-1}$ )	$\mu_h$ ( $\text{cm}^2 \text{V}^{-1} \text{s}^{-1}$ )	$I_{on}/I_{off}$	$V_{th}$ (V)
PPTDPP-OD-HE	BG-BC	Au	$\text{SiO}_2$		$\sim 10^4$	$10^2$	-21
PPTDPP-OD-TEG	BG-BC	Au	$\text{SiO}_2$	$10^{-3}$	$10^{-3}$	$10^3$	$\pm 17$
2DPP-OD-HE	BG-BC	Au	$\text{SiO}_2$		$8 \times 10^{-4}$	$10^3$	-15.2
2DPP-OD-TEG	BG-BC	Au	$\text{SiO}_2$	$10^{-2}$	$10^{-2}$	$10^4$	$< \pm 10$

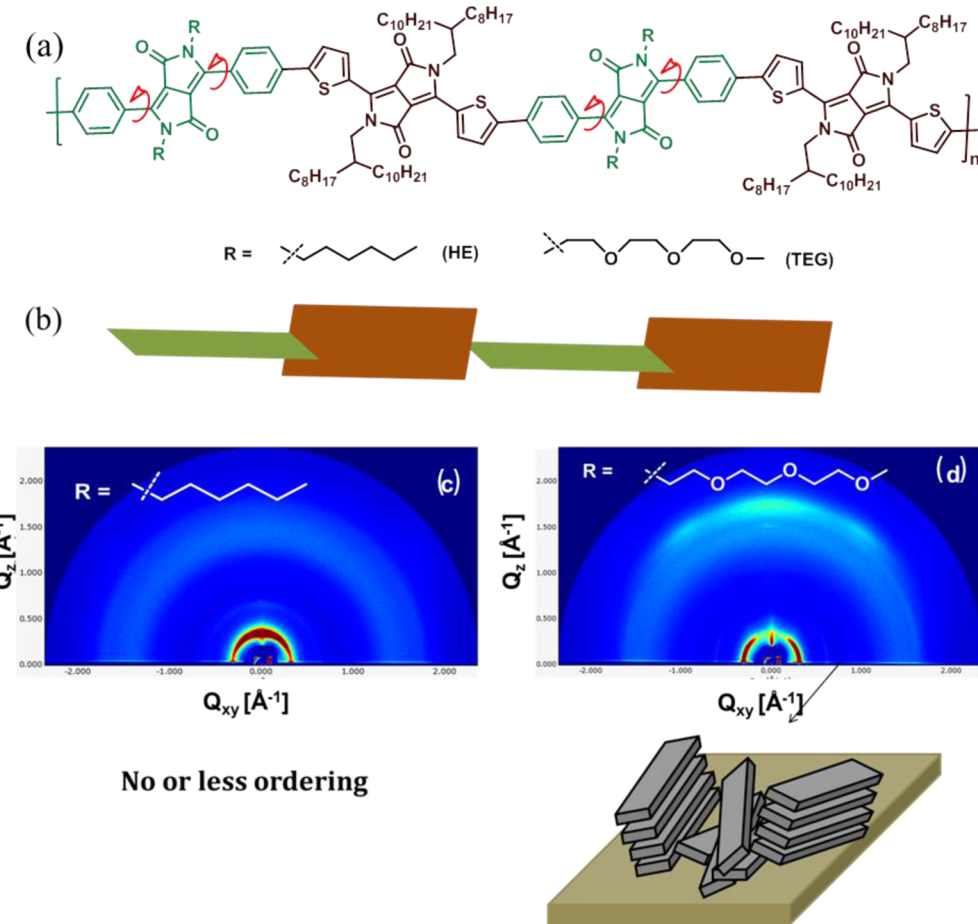


**Figure 8.** GIXD pattern of as-spun (c) PPTDPP-OD-HE and (d) PPTDPP-OD-TEG thin films.

carrier mobilities were obtained from the polymers with *n*-hexyl and triethylene glycol side chains, but a difference in the threshold voltage was shown. Transistors based on 2DPP-OD-HE show a slightly lower threshold voltage ( $V_{th}$ ) of -15.2 V as compared to PPTDPP-OD-HE-based transistors (approximately -21 V). As compared to the phenyl DPP-based

polymers PPTDPP-OD-HE and PPTDPP-OD-TEG, thiophene DPP-based polymers 2DPP-OD-HE and 2DPP-OD-TEG exhibited higher charge carrier mobilities and smaller threshold voltages as presented in Table 3. This shows that a higher torsional angle in PDPP-based polymers inhibits strong intermolecular interactions and increases the number of trap

sites in PPTDPP-OD-HE thin films as compared to 2DPP-OD-HE films. A similar trend was observed in transistors based on the polymers PPTDPP-OD-TEG and 2DPP-OD-TEG substituted with triethylene glycol side chains.

**Grazing Incidence X-ray Diffraction Studies.** Grazing incidence X-ray diffraction (GIXD) was performed to understand the effect of varying torsional angles on the morphology of the thin films. The GIXD patterns for as-spun PPTDPP-OD-HE and PPTDPP-OD-TEG thin films are shown in Figure 8. The diffractogram for PPTDPP-OD-HE shows randomly oriented film due to the significant arching as shown in Figure 8c. The PPTDPP-OD-TEG films exhibit a highly misaligned face-on orientation with a minor edge-on orientation (Figure 8d).

In contrast to the phenyl DPP-based polymers, thiophene-based DPP polymers show a vertical alignment along the (*h*00) Bragg peaks. The alignment corresponds to a lamellar structure with an edge-on molecular orientation. As a result of reduced torsion, 2DPP-OD-HE and 2DPP-OD-TEG exhibit long-range ordering and adopt a favorable orientation where the  $\pi$ -stacking is parallel to the substrate. The thiophene-based polymers, 2DPP-OD-HE and 2DPP-OD-TEG, showed an enhancement in the charge transport properties<sup>27</sup> due to their edge-on orientation as compared to phenyl-based polymers PPTDPP-OD-HE and PPTDPP-OD-TEG, which adopt a nonfavorable “face-on” orientation. However, we make a note that the unfavorable orientation of these polymers is not suitable for OFET devices, but these materials studied here may be relevant for vertical devices such as organic photovoltaics (OPV) where such orientations are preferred. The testing of these materials for OPV devices is under progress in our laboratory.

## CONCLUSIONS

We have synthesized diketopyrrolopyrrole-based conjugated copolymers with varying torsional angles. In this work, we emphasize the key role of torsional angle on the photophysical and charge transport properties of DPP-based conjugated polymers. The optical properties of the copolymers indicate twist introduced into the polymer backbone leads to poor  $\pi$ -conjugation within the donor–acceptor subunits and acts as structural disorder. The results obtained from GIXD studies evidenced these conformational disorders effect the solid-state packing and  $\pi$ – $\pi$  stacking interactions. The charge carrier mobility obtained from organic field-effect transistor manifests the torsional defects. Larger hysteresis and higher threshold voltages with lower charge carrier mobilities were observed in the output characteristics of phenyl DPP-based polymer PPTDPP-OD-TEG as compared to the thiophene DPP-based polymer 2DPP-OD-TEG, indicating the impact of conformational disorder. The results shown here highlight the importance of structural disorder in a family of DPP-based copolymer and indicate that such defects are decisive in determining the charge transport properties.

## ASSOCIATED CONTENT

### Supporting Information

Materials, experimental details, additional spectra, and device fabrication details. This material is available free of charge via the Internet at <http://pubs.acs.org>.

## AUTHOR INFORMATION

### Corresponding Author

\*Tel.: +91-80-22932651. Fax: +91-80-23601310. E-mail: satish@sscu.iisc.ernet.in.

### Notes

The authors declare no competing financial interest.

## ACKNOWLEDGMENTS

We acknowledge financial support from the Department of Science and Technology, India, through the Indo-UK Apex Program and Ministry of Communication and Information Technology under a grant for the Centre of Excellence in Nanoelectronics, Phase II. E.K.B. and A.L.B. acknowledge the National Science Foundation for their support (DMR-1112455). GIXD was carried out at Stanford Synchrotron Light Source (SSRL).

## REFERENCES

- (1) Darling, S. B.; You, F. The Case for Organic Photovoltaics. *RSC Adv.* **2013**, *3*, 17633–17648.
- (2) Hwang, I.; Scholes, G. D. Electronic Energy Transfer and Quantum-Coherence in pi-Conjugated Polymers. *Chem. Mater.* **2011**, *23*, 610–620.
- (3) Karpen, A.; Choi, C. H.; Kertesz, M. Single-Bond Torsional Potentials in Conjugated Systems: A Comparison of ab Initio and Density Functional Results. *J. Phys. Chem. A* **1997**, *101*, 7426–7433.
- (4) Cacelli, I.; Prampolini, G. Torsional Barriers and Correlations between Dihedrals in p-Polyphenyls. *J. Phys. Chem. A* **2003**, *107*, 8665–8670.
- (5) McCulloch, B.; Ho, V.; Hoarfrost, M.; Stanley, C.; Do, C.; Heller, W. T.; Segalman, R. A. Polymer Chain Shape of Poly(3-alkylthiophenes) in Solution Using Small-Angle Neutron Scattering. *Macromolecules* **2013**, *46*, 1899–1907.
- (6) Vujanovich, E. C.; Bloom, J. W. G.; Wheeler, S. E. Impact of Neighboring Chains on Torsional Defects in Oligothiophenes. *J. Phys. Chem. A* **2012**, *116*, 2997–3003.
- (7) Darling, S. B. Isolating the Effect of Torsional Defects on Mobility and Band Gap in Conjugated Polymers. *J. Phys. Chem. B* **2008**, *112*, 8891–8895.
- (8) Hu, D.; Yu, J.; Wong, K.; Bagchi, B.; Rossky, P. J.; Barbara, P. F. Collapse of Stiff Conjugated Polymers with Chemical Defects into Ordered, Cylindrical Conformations. *Nature* **2000**, *405*, 1030–1033.
- (9) Tsao, H. N.; Cho, D. M.; Park, I.; Hansen, M. R.; Mavrinckiy, A.; Yoon, D. Y.; Graf, R.; Pisula, W.; Spiess, H. W.; Mullen, K. Ultrahigh Mobility in Polymer Field-Effect Transistors by Design. *J. Am. Chem. Soc.* **2011**, *133*, 2605–2612.
- (10) Bounos, G.; Ghosh, S.; Lee, A. K.; Plunkett, K. N.; DuBay, K. H.; Bolinger, J. C.; Zhang, R.; Friesner, R. A.; Nuckolls, C.; Reichman, D. R.; et al. Controlling Chain Conformation in Conjugated Polymers Using Defect Inclusion Strategies. *J. Am. Chem. Soc.* **2011**, *133*, 10155–10160.
- (11) Bolinger, J. C.; Traub, M. C.; Brazard, J.; Adachi, T.; Barbara, P. F.; Vanden Bout, D. A. Conformation and Energy Transfer in Single Conjugated Polymers. *Acc. Chem. Res.* **2012**, *45*, 1992–2001.
- (12) Adachi, T.; Brazard, J.; Ono, R. J.; Hanson, B.; Traub, M. C.; Wu, Z.-Q.; Li, Z.; Bolinger, J. C.; Ganesan, V.; Bielawski, C. W.; et al. Regioregularity and Single Polythiophene Chain Conformation. *J. Phys. Chem. Lett.* **2011**, *2*, 1400–1404.
- (13) Bronstein, H.; Chen, Z. Y.; Ashraf, R. S.; Zhang, W. M.; Du, J. P.; Durrant, J. R.; Tuladhar, P. S.; Song, K.; Watkins, S. E.; Geerts, Y.; et al. Thieno 3,2-b thiophene-Diketopyrrolopyrrole-Containing Polymers for High-Performance Organic Field-Effect Transistors and Organic Photovoltaic Devices. *J. Am. Chem. Soc.* **2011**, *133*, 3272–3275.
- (14) Bijleveld, J. C.; Gevaerts, V. S.; Di Nuzzo, D.; Turbiez, M.; Mathijssen, S. G. J.; de Leeuw, D. M.; Wienk, M. M.; Janssen, R. A. J.

Efficient Solar Cells Based on an Easily Accessible Diketopyrrolopyrrole Polymer. *Adv. Mater.* **2010**, *22*, E242–E246.

(15) Dou, L. T.; Gao, J.; Richard, E.; You, J. B.; Chen, C. C.; Cha, K. C.; He, Y. J.; Li, G.; Yang, Y. Systematic Investigation of Benzodithiophene- and Diketopyrrolopyrrole-Based Low-Bandgap Polymers Designed for Single Junction and Tandem Polymer Solar Cells. *J. Am. Chem. Soc.* **2012**, *134*, 10071–10079.

(16) Tang, C. W. 2-Layer Organic Photovoltaic Cell. *Appl. Phys. Lett.* **1986**, *48*, 183–185.

(17) Dou, L. T.; Chang, W. H.; Gao, J.; Chen, C. C.; You, J. B.; Yang, Y. A Selenium-Substituted Low-Bandgap Polymer with Versatile Photovoltaic Applications. *Adv. Mater.* **2013**, *25*, 825–831.

(18) Liang, Y.; Yu, L. A New Class of Semiconducting Polymers for Bulk Heterojunction Solar Cells with Exceptionally High Performance. *Acc. Chem. Res.* **2010**, *43*, 1227–1236.

(19) Naik, M. A.; Patil, S. Diketopyrrolopyrrole-Based Conjugated Polymers and Small Molecules for Organic Ambipolar Transistors and Solar Cells. *J. Polym. Sci., Part A: Polym. Chem.* **2013**, *51*, 4241–4260.

(20) Dou, L. T.; You, J. B.; Yang, J.; Chen, C. C.; He, Y. J.; Murase, S.; Moriarty, T.; Emery, K.; Li, G.; Yang, Y. Tandem Polymer Solar Cells Featuring a Spectrally Matched Low-Bandgap Polymer. *Nat. Photonics* **2012**, *6*, 180–185.

(21) Woo, C. H.; Beaujuge, P. M.; Holcombe, T. W.; Lee, O. P.; Frechet, J. M. J. Incorporation of Furan into Low Band-Gap Polymers for Efficient Solar Cells. *J. Am. Chem. Soc.* **2010**, *132*, 15547–15549.

(22) Li, J.; Zhao, Y.; Tan, H. S.; Guo, Y. L.; Di, C. A.; Yu, G.; Liu, Y. Q.; Lin, M.; Lim, S. H.; Zhou, Y. H. A Stable Solution-Processed Polymer Semiconductor with Record High-Mobility for Printed Transistors. *Sci. Rep.* **2012**, *2*, 754.

(23) Bloking, J. T.; Han, X.; Higgs, A. T.; Kastrop, J. P.; Pandey, L.; Norton, J. E.; Risko, C.; Chen, C. E.; Bredas, J. L.; McGehee, M. D.; et al. Solution-Processed Organic Solar Cells with Power Conversion Efficiencies of 2.5% using Benzothiadiazole/Imide-Based Acceptors. *Chem. Mater.* **2011**, *23*, 5484–5490.

(24) Sirringhaus, H.; Brown, P. J.; Friend, R. H.; Nielsen, M. M.; Bechgaard, K.; Langeveld-Voss, B. M. W.; Spiering, A. J. H.; Janssen, R. A. J.; Meijer, E. W.; Herwig, P.; et al. Two-Dimensional Charge Transport in Self-Organized, High-Mobility Conjugated Polymers. *Nature* **1999**, *401*, 685–688.

(25) Kang, I.; Yun, H. J.; Chung, D. S.; Kwon, S. K.; Kim, Y. H. Record High Hole Mobility in Polymer Semiconductors via Side-Chain Engineering. *J. Am. Chem. Soc.* **2013**, *135*, 14896–14899.

(26) Guo, X.; Puniredd, S. R.; Baumgarten, M.; Pisula, W.; Mullen, K. Benzotriphosphine-Based Donor-Acceptor Copolymers with Distinct Supramolecular Organizations. *J. Am. Chem. Soc.* **2012**, *134*, 8404–8407.

(27) Kanimozhi, C.; Yaacobi-Gross, N.; Chou, K. W.; Amassian, A.; Anthopoulos, T. D.; Patil, S. Diketopyrrolopyrrole-Diketopyrrolopyrrole-Based Conjugated Copolymer for High-Mobility Organic Field-Effect Transistors. *J. Am. Chem. Soc.* **2012**, *134*, 16532–16535.

(28) Bürckstümmer, H.; Weissenstein, A.; Bialas, D.; Würthner, F. Synthesis and Characterization of Optical and Redox Properties of Bithiophene-Functionalized Diketopyrrolopyrrole Chromophores. *J. Org. Chem.* **2011**, *76*, 2426–2432.

(29) Rabindranath, A. R.; Zhu, Y.; Heim, I.; Tieke, B. Red Emitting N-Functionalized Poly(1,4-diketo-3,6-diphenylpyrrolo[3,4-c]pyrrole) (Poly-DPP): A Deeply Colored Polymer with Unusually Large Stokes Shift. *Macromolecules* **2006**, *39*, 8250–8256.

(30) Dhar, J.; Venkatramaiah, N.; A, A.; Patil, S. Photophysical, Electrochemical and Solid State Properties of Diketopyrrolopyrrole Based Molecular Materials: Importance of the Donor Group. *J. Mater. Chem. C* **2014**, *2*, 3457–3466.

(31) Sonar, P.; Singh, S. P.; Li, Y.; Soh, M. S.; Dodabalapur, A. A Low-Bandgap Diketopyrrolopyrrole-Benzothiadiazole-Based Copolymer for High-Mobility Ambipolar Organic Thin-Film Transistors. *Adv. Mater.* **2010**, *22*, 5409–5413.